

**Asymmetry observables in  $e^+e^- \rightarrow \pi^+\pi^-\gamma$  in the  $\phi$  region within a chiral unitary approach**

L. Roca

*Departamento de Física, Universidad de Murcia, E-30071, Murcia, Spain*

E. Oset

*Departamento de Física Teórica and IFIC, Centro Mixto Universidad de Valencia-CSIC, Institutos de Investigación de Paterna, Apartado 22085, 46071 Valencia, Spain*

(Received 5 November 2009; published 14 January 2010)

We make a theoretical study of the charge and forward-backward pion asymmetries in the  $e^+e^- \rightarrow \pi^+\pi^-\gamma$  process on and off the  $\phi$  resonance energy. These observables are rather sensitive to the inner details of the theoretical models to describe the reaction. In addition to the standard implementation of the initial state radiation and the bremsstrahlung contribution to the final state radiation, we use the techniques of the chiral unitary approach to evaluate the contribution from the mechanisms of  $\phi$  decay into  $\pi^+\pi^-\gamma$ . This contribution involves the implementation of final state interaction from direct chiral loops, the exchange of vector and axial-vector resonances and the final state interaction through the consideration of the meson-meson unitarized amplitudes, which were found important in a previous work describing the  $\phi \rightarrow \pi\pi\gamma$ . We find a good reproduction of the experimental data from KLOE for the forward-backward asymmetry, both at the  $\phi$  peak and away from it. We also make predictions for the angular distributions of the charge asymmetry and show that this observable is very sensitive to the chiral loops involved in  $\phi$  radiative decay.

DOI: [10.1103/PhysRevD.81.014010](https://doi.org/10.1103/PhysRevD.81.014010)

PACS numbers: 13.25.Jx, 12.39.Fe, 13.66.Bc

**I. INTRODUCTION**

The radiative decays of the  $\phi$  into  $\pi\pi\gamma$  has been considered as one of the most suitable reactions to get information about the  $f_0(980)$  resonance [1–14]. In the last decade the idea that this resonance, as well as the other light scalar resonances,  $a_0(980)$ ,  $f_0(600)$  or  $\kappa(800)$ , are dynamically generated from multiple scattering using the ordinary chiral Lagrangians [15–18] has shed new light into the problem of the nature of the scalar mesons. From the experimental point of view, both the CM2 Collaboration at Novosibirsk [19] and the KLOE Collaboration of the  $\phi$  factory DAΦNE at Frascati [20] reported results on the two pion invariant mass distribution in the  $\phi \rightarrow \pi^0\pi^0\gamma$  decay. The  $\phi$  meson is produced from electron-positron collision. In the study of the charged pion channel,  $\phi \rightarrow \pi^+\pi^-\gamma$ , the problem of the large contribution of the initial state radiation (ISR) (where the photon is emitted from the electron or the positron, not possible in the  $\pi^0\pi^0\gamma$  case for charge parity reasons), can turn itself into an advantage through the analysis of different asymmetry observables, like the so-called forward-backward pion asymmetry and charge asymmetry [21,22]. The reason is that this observable can be very sensitive to inner details of the models to describe the reaction, thanks to the importance of the interference between the final state radiation (FSR) and the ISR mechanisms. The former is very model dependent and thus the study of this asymmetry is a good tool to test models for the FSR. In particular, if the  $e^+e^-$  center of mass energy is set to the  $\phi(1020)$  peak, as is the case of DAΦNE, it is very suited to test  $\phi$  decay

models where the scalar mesons play a crucial role, particularly the  $f_0(980)$  resonance.

For the FSR in the  $e^+e^- \rightarrow \pi^+\pi^-\gamma$  reaction, there are some standard models like the scalar QED for the final state bremsstrahlung process [21–25]. This is the most important contribution for large invariant mass of the pions, but for the lowest part of the two pion spectrum other mechanisms related to  $\phi$  radiative decay become competitive. In [23,24,26] a correction from the vector contribution using the resonance chiral theory Lagrangians [27] was also considered. For the  $\phi$  decay process there is a wider variety of models which differ on the treatment of the scalar mesons. Reference [28] considers the contribution of intermediate scalars using a point-like  $\phi f_0\gamma$  interaction with explicit scalar meson fields. In Refs. [24,29] the double resonance contribution  $e^+e^- \rightarrow \phi \rightarrow \rho^\pm\pi^\pm \rightarrow \pi^+\pi^-\gamma$  was also considered. The most recent approach to the problem [26] treats the scalar mesons from kaon loops using the techniques of the chiral unitary approach to generate dynamically the scalar resonances and compare the results with other models of scalar mesons like the linear sigma model [30]. The authors in [26] could not find a good reproduction of the KLOE data [31] on the asymmetry in the whole double pion mass range.<sup>1</sup> In Ref. [10], a very elaborate model was developed for the  $\phi$  decay into  $\pi\pi\gamma$ . The model considered the implementation of the two pseudoscalar final state interac-

<sup>1</sup>Recently the authors of Ref. [26] communicated to us that their results in the low energy region will be modified due to the numerics.

tion (FSI) using the techniques of the chiral unitary approach, both from the kaon loops and from the production through the exchange of intermediate vector and axial-vector resonances. These new mechanisms were shown to be relevant for the two pion mass distribution in the  $\phi$  radiative decay, specially at the low part of the spectrum.

The aim of this work is to evaluate the forward-backward and charge asymmetries in the  $e^+e^- \rightarrow \pi^+\pi^-\gamma$  reaction in order to test the accuracy of the model used in Ref. [10] to evaluate the  $\phi\pi\pi\gamma$  decay. This provides an extra test on the chiral unitary approach and its repercussion on the dynamical generation of the light scalar mesons.

## II. FORMALISM FOR $e^+e^- \rightarrow \pi^+\pi^-\gamma$

The  $e^+e^- \rightarrow \pi^+\pi^-\gamma$  gets contribution from two different processes depending on where the photon is emitted: the ISR and the FSR. In the ISR the radiated photon is emitted from the initial electron or positron and it just involves a trivial electromagnetic process except for the coupling of the pion to the photon which can be accounted for by the pion form factor. In the FSR the final photon is emitted after the virtual photon attached to the electron-positron line and it is the most model dependent part. For a diagrammatic representation of the final diagrams for the ISR we refer to Figs. (1a) and (1b) of Ref. [29].

The amplitude for the FSR process can be decomposed in a model independent way in terms of three different structure functions. For this decomposition we follow the formalism of Ref. [23] which is also used in Ref. [26] (see Ref. [23] for further details). We summarize it briefly in this section.

For the  $e^-(p_1)e^+(p_2) \rightarrow \pi^+(p_+)\pi^-(p_-)\gamma(k)$  it is convenient to introduce the variables  $Q = p_+ + p_-$ ,  $q = p_+ + p_-$ ,  $l = p_+ - p_-$  and five independent Lorentz scalars defined as

$$\begin{aligned} s &\equiv Q^2 = 2p_1 \cdot p_2, & t_1 &\equiv (p_1 - k)^2 = -2p_1 \cdot k, \\ t_2 &\equiv (p_2 - k)^2 = -2p_2 \cdot k, & u_1 &\equiv l \cdot p_1, \\ u_2 &\equiv l \cdot p_2. \end{aligned} \quad (1)$$

(The electron mass is neglected in the present work.)

As mentioned above, the total amplitude can be decomposed as

$$T = T_{\text{ISR}} + T_{\text{FSR}} \quad (2)$$

with

$$T_{\text{ISR}} = -\frac{e}{q^2} L^{\mu\nu} \epsilon_\nu^* l_\mu F_\pi(q^2), \quad (3)$$

$$T_{\text{FSR}} = \frac{e^2}{s} J_\mu T_F^{\mu\nu} \epsilon_\nu^*, \quad (4)$$

where

$$\begin{aligned} L^{\mu\nu} &= e^2 \bar{u}_{s_2}(-p_2) \left[ \gamma^\nu \frac{(-\not{p}_2 + \not{k} + m_e)}{t_2} \gamma^\mu \right. \\ &\quad \left. + \gamma^\mu \frac{(\not{p}_1 - \not{k} + m_e)}{t_1} \gamma^\nu \right] u_{s_1}(p_1), \end{aligned} \quad (5)$$

$$J_\mu = e \bar{u}_{s_2}(-p_2) \gamma_\mu u_{s_1}(p_1). \quad (6)$$

In Eq. (3),  $F_\pi(q^2)$  is the pion form factor which we take in the present work from Ref. [23].

As explained in Ref. [24], the most general form of the FSR tensor  $T_F^{\mu\nu}$  can be written as

$$T_F^{\mu\nu} = f_1 \tau_1^{\mu\nu} + f_2 \tau_2^{\mu\nu} + f_3 \tau_3^{\mu\nu}, \quad (7)$$

where the  $\tau_i^{\mu\nu}$  are

$$\begin{aligned} \tau_1^{\mu\nu} &= k^\mu Q^\nu - g^{\mu\nu} k \cdot Q, \\ \tau_2^{\mu\nu} &= k \cdot l (l^\mu Q^\nu - g^{\mu\nu} k \cdot l) + l^\nu (k^\mu k \cdot l - l^\mu k \cdot Q), \\ \tau_3^{\mu\nu} &= Q^2 (g^{\mu\nu} k \cdot l - k^\mu l^\nu) + Q^\mu (l^\nu k \cdot Q - Q^\nu k \cdot l). \end{aligned} \quad (8)$$

The theoretical models to describe the FSR can then concentrate on evaluating the Lorentz scalar functions,  $f_i$ .

The cross section for the  $e^+e^- \rightarrow \pi^+\pi^-\gamma$  reaction, with normalization  $\bar{u}_{s'} u_s = 2m_e \delta_{s's'}$ , can be written as

$$\begin{aligned} \sigma &= \frac{1}{16s(2\pi)^4} \int d\omega_+ \int d\omega_- \int d\cos\theta_+ \int d\phi_{+-} |T|^2 \\ &\quad \times \Theta(1 - B^2) \end{aligned} \quad (9)$$

where  $\omega_{+(-)}$  is the energy of the  $\pi_{+(-)}$ ,  $\theta_+$  is the  $\pi^+$  polar angle,  $\phi_{+-}$  is the azimuthal angle of the  $\pi^-$  considering as  $z$  axis the  $\pi^+$  direction,  $\Theta(x)$  is the step function and  $B$  is given by

$$B = \frac{(\sqrt{s} - \omega_+ - \omega_-)^2 - |\vec{p}_+|^2 - |\vec{p}_-|^2}{2|\vec{p}_+||\vec{p}_-|}. \quad (10)$$

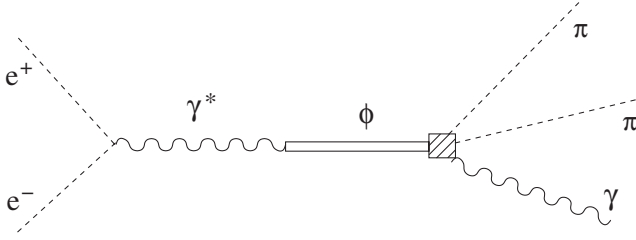
The total amplitude squared,  $|T|^2$ , can be explicitly separated into the contributions on the ISR, the FSR and the interference of the two amplitudes:

$$|T|^2 = |T_{\text{ISR}}|^2 + |T_{\text{FSR}}|^2 + 2 \text{Re}\{T_{\text{ISR}} T_{\text{FSR}}^*\}. \quad (11)$$

Because of charge parity ( $C$ ) conservation, the final pion pair must be in a  $C = -1$  ( $+1$ ) state for the ISR (FSR) case. The interference between two terms with opposite  $C$  parity is  $C$ -odd and, then, it changes sign under the interchange of the two charged pions. Therefore, it produces a charge asymmetry, and also a forward-backward asymmetry

$$A_{\text{FB}} = \frac{N(\theta_+ > 90^\circ) - N(\theta_+ < 90^\circ)}{N(\theta_+ > 90^\circ) + N(\theta_+ < 90^\circ)}, \quad (12)$$

where we consider  $\theta_+$  defined with respect to the positron beam, and  $N$  represents the number of  $\pi^+$  events in the given angular region.

FIG. 1. Mechanism involving the  $\phi(1020)$  decay.

### III. UNITARY CHIRAL PERTURBATION THEORY MODEL TO THE $\phi$ CONTRIBUTION TO THE FSR

The expression of  $|T_{\text{ISR}}|^2$ ,  $|T_{\text{FSR}}|^2$  and  $\text{Re}\{T_{\text{ISR}}T_{\text{FSR}}^*\}$  of Eq. (11) in terms of the structure functions  $f_i$  of Eq. (7) can be found in Eqs. (8), (17) and (25) of Ref. [23]. For the bremsstrahlung process we use Eqs. (11)–(20) of Ref. [24], which correspond to the Feynman diagrams shown in Fig. 2 of Ref. [23].

For  $e^+e^-$  center of mass energies very close to the mass of the  $\phi(1020)$  resonance, the mechanisms producing a  $\phi$  meson from the virtual photon and its subsequent decay into  $\pi^+\pi^-\gamma$  are relevant (see Fig. 1).

The diagrams for the different contributions to the  $\phi$  decay are shown in Fig. 2.

This model contains, in a first place, the loops coming from  $\phi \rightarrow K^+K^-$  decay and the implementation of the final state interaction of the pions using the techniques of the chiral unitary approach [8] [Fig. 2(a)]. This mechanism was also considered in Ref. [26] using the resonance chiral perturbation theory Lagrangians. In the present work we use the Lagrangians of the hidden gauge symmetry [32–34], where the conversion of the photons to vector mesons is a natural consequence of the general Lagrangians. Their use is equivalent to working with the scheme of [8,10,26] imposing the results of vector meson dominance [35], essentially  $F_V = 2G_V$ .

This mechanism contributes only to the  $f_1$  function and is given by

$$f_1 = -\frac{4}{3\sqrt{3}}D_\phi(Q^2)M_V^2\tilde{G}(\sqrt{s}, M_I)\frac{1}{Q^2 - M_I^2}t_{KK,\pi\pi}^{I=0}(M_I) \quad (13)$$

where  $M_I \equiv \sqrt{q^2}$  is the final two pion invariant mass,  $\tilde{G}(\sqrt{s}, M_I)$  is the three meson loop function given in [10],  $D_\phi$  is the  $\phi$  meson propagator and  $t_{KK,\pi\pi}^{I=0}$  is the  $s$ -wave isospin  $I = 0$   $K\bar{K} \rightarrow \pi\pi$  unitarized scattering amplitude in the normalization of [15]. Note that the main difference with respect to [26] or the expression given in [8,10] is the term proportional to  $F_V/2 - G_V$  which is zero in vector meson dominance, implicit in the hidden gauge symmetry (HGS) Lagrangians, and contributes very little if explicitly considered [8,26]. It is worth mentioning that the meson-meson unitarized amplitude generates also the  $\sigma(500)$

contribution apart from the  $f_0(980)$  one, without the need to include explicit fields for these scalar resonances. They appear just from the implementation of unitarity from the lowest order meson-meson chiral Lagrangian [15–17]. Even more, it provides the actual shape of the amplitude in the real axis (with its possible background, etc.), not just the pole contribution. The full gauge invariant set of diagrams in Fig. 2(a) requires also a term where the photon couples to the four meson vertex. However, using the method of Ref. [36] one does not need to evaluate its contribution explicitly [36–39].

The model [10] adds to the previous mechanisms the contribution from the intermediate exchange of vector and axial-vector mesons [Figs. 2(b)–2(f)]. The vector meson exchange was also included, but only at tree level [Fig. 2(b)], in [23,24,26,29] in a different way. In [10] the  $\phi$  couples to  $\rho\pi$  through  $\phi\omega$  mixing since a direct coupling is OZI suppressed. The exchange of axial-vector mesons was also included in [10] but the amplitude at tree level [Fig. 2(c)] is typically about 2 orders of magnitude smaller than the one for the vector meson exchange at tree level due to the fact that the exchanged  $b_1$  is very off shell. Therefore, its contribution is negligible, but we include it in our model for consistency.

In our formalism, the contribution of the tree level vector meson exchange [Fig. 2(b)] to the structure functions is given by

$$\begin{aligned} f_1 &= \alpha[D_\rho(P_\rho)(l^2 + Q \cdot k - 2k \cdot l) \\ &\quad + D_\rho(P'_\rho)(l^2 + Q \cdot k + 2k \cdot l)] \\ f_2 &= -\alpha[D_\rho(P_\rho) + D_\rho(P'_\rho)] \\ f_3 &= -\alpha[D_\rho(P_\rho) - D_\rho(P'_\rho)] \end{aligned} \quad (14)$$

with

$$\alpha = -C\tilde{\epsilon}\frac{M_V^2}{9\sqrt{2}}\frac{f^2G^2}{M_\omega^2}D_\phi(Q^2). \quad (15)$$

See Ref. [10] for further details on the definition and values of the different constants of Eq. (15). In Eq. (14)  $P_\rho = (Q - l + k)/2$  and  $P'_\rho = (Q + l + k)/2$ .

One of the main novelties of the work [10] was the implementation of the final meson-meson scattering in the mechanisms involving the vector and axial-vector exchange [Figs. 2(d)–2(f)]. These mechanisms modified significantly the shape of the double pion mass distribution in the  $\phi$  decay spectrum [10]. In addition to the loop mechanism constructed from the exchange of the  $\rho$  meson [Fig. 2(d)], it is also possible to implement the loops in mechanisms with exchange of vector  $K^*$  [Fig. 2(e)] and axial-vector resonances,  $K_1(1270)$  and  $K_1(1400)$  [Fig. 2(f)].



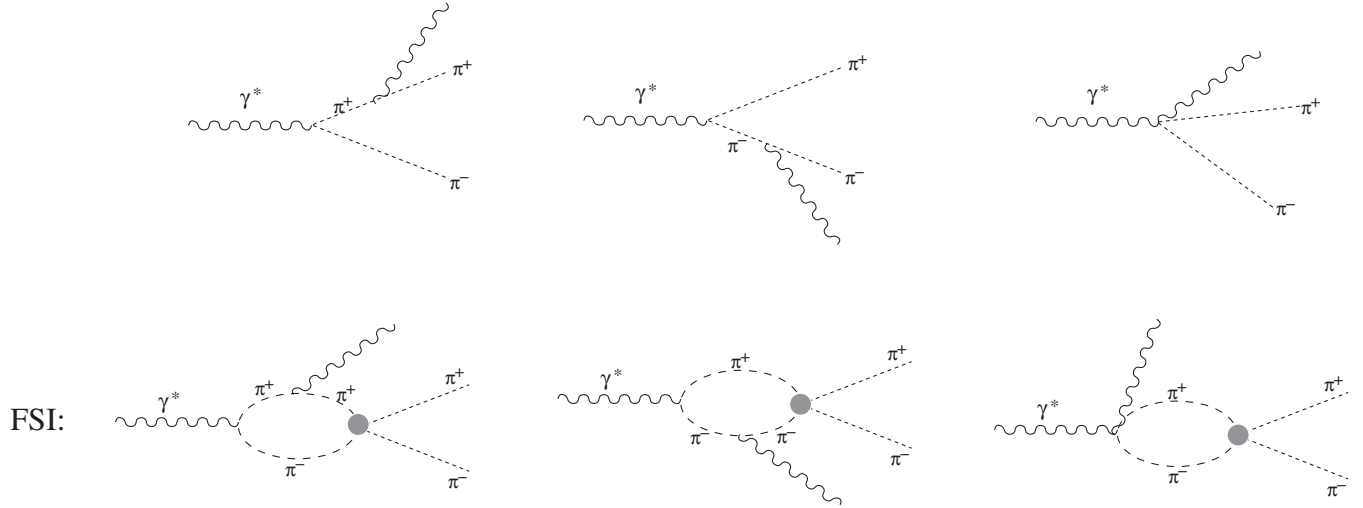


FIG. 3. Dominant contribution to the final pion bremsstrahlung process, where the final state interaction is implemented.

nisms contribute only to the  $f_1$  function and they give

$$f_1 = i \frac{8}{3} \frac{1}{Q^2 - M_I^2} (G_{\pi\pi} - \tilde{G}(\sqrt{s}, M_I)) t_{\pi\pi, \pi\pi}^{I=0}(M_I) F_\pi(Q^2), \quad (16)$$

where  $t_{\pi\pi, \pi\pi}^{I=0}$  is the  $s$ -wave isospin  $I = 0$   $\pi\pi \rightarrow \pi\pi$  unitarized scattering amplitude in the normalization of [15].

#### IV. RESULTS

In order to compare with the experimental data of [31,40], we implement in our theoretical calculations the same cuts as in the KLOE experiment. Thus, we account only for pions with angles in the region  $45^\circ < \theta_\pm < 135^\circ$ , and photons with  $45^\circ < \theta_\gamma < 135^\circ$  and  $E_\gamma > 10$  MeV.

In Fig. 4 we show the results for the forward-backward asymmetry as a function of the two pion invariant mass,  $M_I$ , including only the bremsstrahlung process (dashed line); adding the direct chiral loops (dotted line); adding the vector meson exchange at tree level (dash-dotted line); adding the loops from the vector and axial-vector exchange (double-dash-dotted line) and the full model which includes also the FSI in the bremsstrahlung process (solid line).

The sudden drop at the end of the spectrum is due to the photon energy cut. At higher invariant masses the dominant contribution is given by the bremsstrahlung process as already obtained in all previous theoretical works on the reaction. The effect of the scalar  $f_0(980)$  resonance is clearly visible as a dip in the invariant mass spectrum. At low invariant masses the sequential exchange of vector mesons has a crucial effect in the final shape of the asymmetry. This mechanism was not considered in Ref. [28] claiming that it was negligible. On the other hand, the implementation of the final loops in the sequential vector and axial-vector meson exchange is less relevant than in

the  $\phi \rightarrow \pi\pi\gamma$  decay [10]. The implementation of the final state interaction in the bremsstrahlung process, which is also a novelty of the present calculation, is negligible at high invariant masses and has a small effect at the lower part of the spectrum except in the region around 400 MeV, where the contribution is more significant due to the strong interferences among the different mechanisms.

If we change the center of mass energy of the electron-positron collision to values off the  $\phi$  peak, the contribution of the  $\phi$  mechanisms is almost completely removed. This is shown in Fig. 5, where we plot the same calculation as in

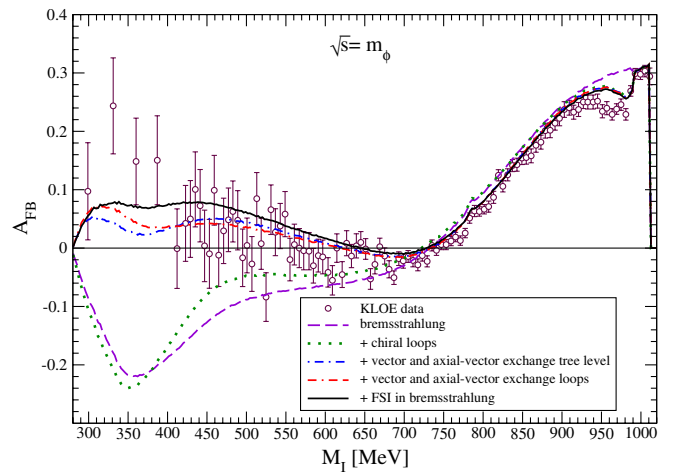


FIG. 4 (color online). Different FSR contributions to the forward-backward asymmetry for electron-positron center of mass energy  $\sqrt{s} = m_\phi$ . Experimental cuts are implemented. Only bremsstrahlung, dashed line; adding the direct chiral loops, dotted line; adding the vector meson exchange at tree level, dash-dotted line; adding the loops from the vector and axial-vector exchange, double-dash-dotted line; full model, which includes also the FSI in the Bremsstrahlung process, solid line. Experimental data from Refs. [31,40].

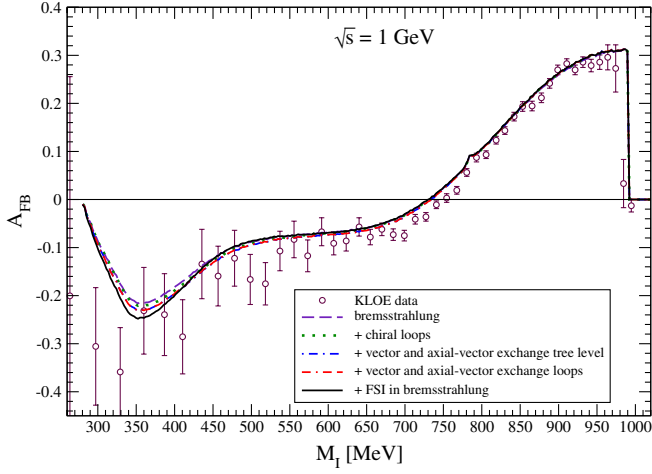


FIG. 5 (color online). Same as Fig. 4 but for  $\sqrt{s} = 1$  GeV. Experimental data from Ref. [40].

Fig. 4 but for  $\sqrt{s} = 1$  GeV instead of  $\sqrt{s} = m_\phi = 1.02$  GeV used in Fig. 4. The experimental data are taken from Ref. [40]. We can see that the standard non- $\phi$  mechanisms suffice to obtain a good agreement with the KLOE data [40]. In order to cancel the  $\phi$  effects it is not necessary to move very much the energy from the  $\phi$  peak since the  $\phi$  resonance is very narrow,  $\sim 4$  MeV. One of the main consequences of removing almost completely the  $\phi$  resonance contribution (Fig. 2) by going to  $\sqrt{s} = 1$  GeV is that the dip due to the  $f_0(980)$  resonance of Fig. 4 is not visible now in our theoretical curve in Fig. 5. This is because in our model the  $f_0(980)$  contribution comes from the final state interaction of meson pairs produced mostly in diagrams implying  $\phi$  production. The implementation of final state interaction in the bremsstrahlung mechanism is very small, as seen in Fig. 5.

Overall, we find a good reproduction of this asymmetry in the whole invariant mass spectrum. The correct predic-

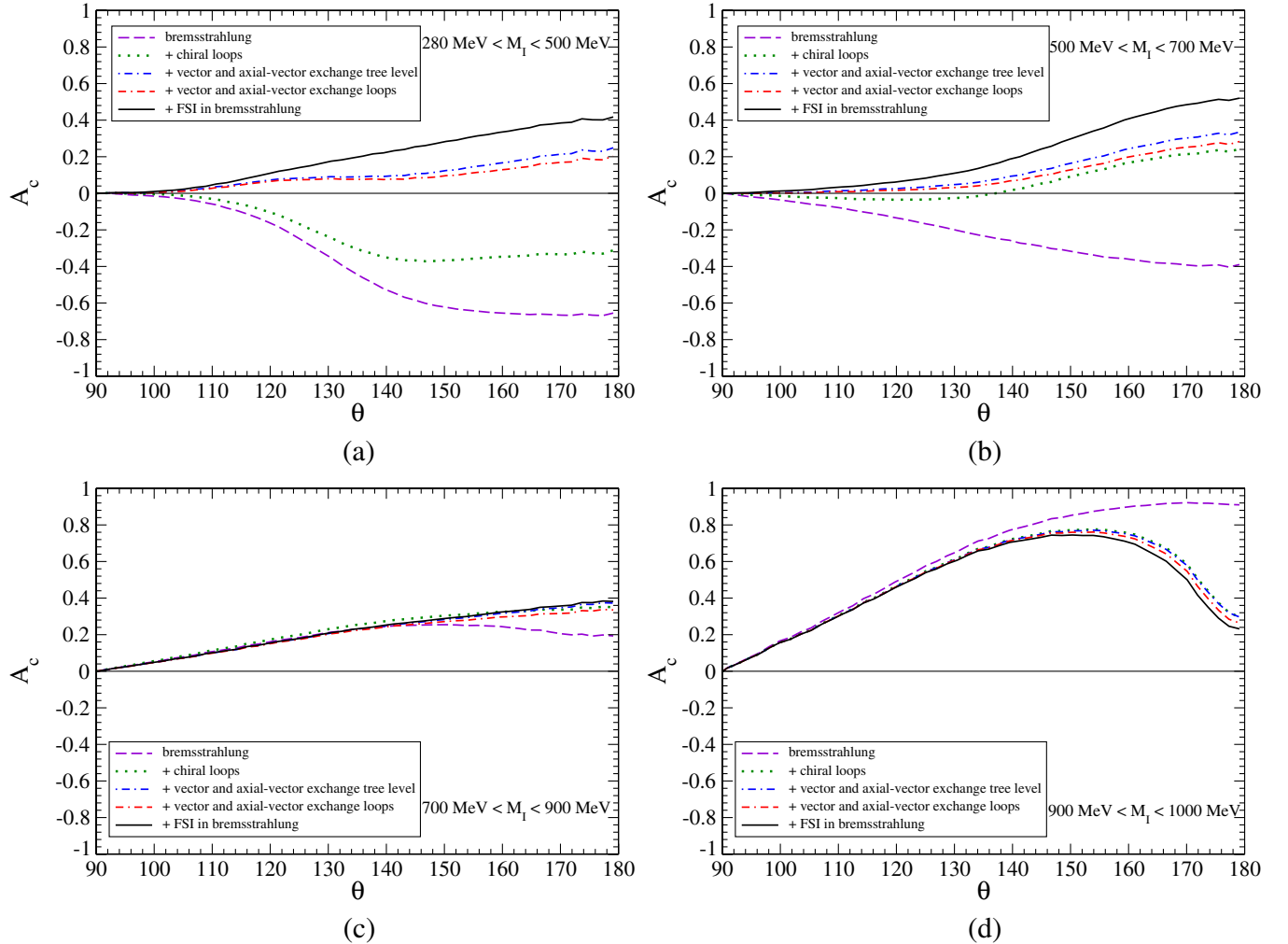


FIG. 6 (color online). Different FSR contributions to the charge asymmetry, Eq. (17), for electron-positron center of mass energy  $\sqrt{s} = m_\phi$ . Experimental cuts for the photons are implemented.

tion of the line shapes on and off the  $\phi$  peak is an important cross-check of the consistency of our approach.

We can use other observables to test the theoretical model and the contribution of the different mechanisms. For instance, like in Ref. [28], we can calculate the charge asymmetry

$$A_c(\theta) = \frac{N_+(\theta) - N_-(\theta)}{N_+(\theta) + N_-(\theta)} \quad (17)$$

where  $N_{+(-)}(\theta)$  is the number of  $\pi^{+(-)}$  emitted in the  $\theta$  direction defined with respect to the positron axis. As discussed after Eq. (11), only the interference term  $\text{Re}\{T_{\text{ISR}}T_{\text{FSR}}^*\}$  changes sign upon the interchange of  $\pi^+$ ,  $\pi^-$ , hence the numerator of Eq. (17) contains only this term in  $|T|^2$ . This asymmetry satisfies  $A_c(\theta) = -A_c(180^\circ - \theta)$ , thus we only plot angles from  $90^\circ$  on. We plot in Fig. 6 the charge asymmetry as a function of the polar angle of the corresponding pion, for different  $\pi\pi$  invariant mass ranges and implementing the KLOE acceptance for the photons. There is no experimental data published on this observable. Again one can see in the figures the strong effect of the vector meson exchange mechanisms at low invariant masses and the  $f_0(980)$  at high masses.

The effect of the chiral loops in  $A_c$  is very important in all ranges of the invariant mass. This effect was not so pronounced for the forward-backward asymmetry. In the range of  $500 \leq M_I \leq 700$  MeV the chiral loops reverse the sign of the  $A_c$  magnitude, something that could be clearly visible with the present KLOE angular acceptance. In the range of  $900 \leq M_I \leq 1000$  MeV the chiral loops reduce considerably the strength of  $A_c$ , particularly close to  $180^\circ$ . The FSI in the bremsstrahlung process has also more effect in the  $A_c$  observable than in the forward-backward asymmetry for the two lowest invariant mass ranges.

In [22,28] it was shown that the observable  $A_c$  is very sensitive to details of the model for  $\phi$  radiative decay used to evaluate the FSR contribution. This is due to the strong interference between the FSR and the ISR mechanisms. For instance, in Ref. [28] results for  $A_c$  were shown for a model with explicit scalar meson fields which depends on an unknown production phase. Different values for this phase produce very different results for  $A_c$ . In this respect, it is important to note that when applying the chiral unitary approach to the present problem we have no freedom in parameters and the results presented here are a neat prediction of the model. Since the chiral unitary approach used is the one that generates dynamically the  $f_0(980)$  and  $f_0(600)$ , an eventual agreement of the experiment

with the predictions would provide extra support for this interpretation of the nature of these resonances.

## V. CONCLUSIONS

We have calculated the different contributions to the forward-backward and charge pion asymmetries in  $e^+e^- \rightarrow \pi^+\pi^-\gamma$ . The main aim has been to test the chiral unitary approach calculation of the  $\phi \rightarrow \pi\pi\gamma$  decay [10]. This model implements the final state interaction from direct  $\phi \rightarrow K\bar{K}$  decay, the sequential exchange of vector and axial-vector resonances at tree level and the final state interaction of the meson pair. This meson-meson rescattering generates the scalar resonances without the need to include them as an explicit degree of freedom.

The results of the present work show that there is a good agreement of our theoretical model with the experimental KLOE data on the forward-backward asymmetry, both on the  $\phi$  peak as well as outside its range. The test done outside the  $\phi$  peak using the data of [40] indicates that one has a good control on the conventional non- $\phi$  mechanisms of initial and final state radiation in  $e^+e^- \rightarrow \pi^+\pi^-\gamma$ . The changes seen in the asymmetry at the  $\phi$  peak can then clearly be attributed to the  $\phi$  radiative decay mechanisms. Yet, these changes, particularly at low  $\pi\pi$  invariant masses where they are more drastic, are mostly due to the sequential vector exchange mechanism at tree level, although in the intermediate range of invariant masses the chiral loops are relevant. From the purpose of finding observables which are very sensitive to these chiral loops, we found even more interesting the charge asymmetry. There we could see that at low invariant masses the chiral loops are important, and in the intermediate range  $500 < M_I < 700$  MeV, they even change the sign of the observable. At higher invariant masses the effects are also remarkable, particularly at angles close to  $180^\circ$ , outside the present range of KLOE.

The present results should encourage experimental efforts to measure the charge asymmetry and other related observables which could shed more light on the nature of the scalar resonances.

## ACKNOWLEDGMENTS

We thank M. Napsuciale and A. Gallegos for helpful discussions. This work is partly supported by DGICYT Contracts No. FIS2006-03438 and No. FPA2007-62777 and the EU Integrated Infrastructure Initiative Hadron Physics Project under Grant Agreement No. 227431.

- [1] A. Bramon, G. Colangelo, P.J. Franzini, and M. Greco, Phys. Lett. B **287**, 263 (1992).
- [2] P.J. Franzini, W. Kim, and J. Lee-Franzini, Phys. Lett. B **287**, 259 (1992).
- [3] G. Colangelo and P.J. Franzini, Phys. Lett. B **289**, 189 (1992).
- [4] N.N. Achasov, V.V. Gubin, and E.P. Solodov, Phys. Rev. D **55**, 2672 (1997).
- [5] A. Bramon, A. Grau, and G. Pancheri, Phys. Lett. B **289**, 97 (1992).
- [6] J.A. Oller, Nucl. Phys. A **714**, 161 (2003).
- [7] A. Bramon, R. Escribano, J.L. Lucio, M.M. Napsuciale, and G. Pancheri, Eur. Phys. J. C **26**, 253 (2002).
- [8] E. Marco, S. Hirenzaki, E. Oset, and H. Toki, Phys. Lett. B **470**, 20 (1999).
- [9] V.E. Markushin, Eur. Phys. J. A **8**, 389 (2000).
- [10] J.E. Palomar, L. Roca, E. Oset, and M.J. Vicente Vacas, Nucl. Phys. A **729**, 743 (2003).
- [11] Yu.S. Kalashnikova, A.E. Kudryavtsev, A.V. Nefediev, C. Hanhart, and J. Haidenbauer, Eur. Phys. J. A **24**, 437 (2005).
- [12] D.V. Bugg, Eur. Phys. J. C **47**, 45 (2006).
- [13] R. Escribano, Phys. Rev. D **74**, 114020 (2006).
- [14] R. Escribano, P. Masjuan, and J. Nadal, Phys. Lett. B **670**, 27 (2008).
- [15] J.A. Oller and E. Oset, Nucl. Phys. A **620**, 438 (1997); **A652**, 407 (1999).
- [16] J.A. Oller, E. Oset, and J.R. Peláez, Phys. Rev. Lett. **80**, 3452 (1998); Phys. Rev. D **59**, 074001 (1999).
- [17] J.A. Oller and E. Oset, Phys. Rev. D **60**, 074023 (1999).
- [18] N. Kaiser, Eur. Phys. J. A **3**, 307 (1998).
- [19] R.R. Akhmetshin *et al.* (CMD-2 Collaboration), Phys. Lett. B **462**, 380 (1999).
- [20] A. Aloisio *et al.* (KLOE Collaboration), Phys. Lett. B **537**, 21 (2002).
- [21] S. Binner, J.H. Kuhn, and K. Melnikov, Phys. Lett. B **459**, 279 (1999).
- [22] H. Czyz, A. Grzelinska, J.H. Kuhn, and G. Rodrigo, Eur. Phys. J. C **27**, 563 (2003).
- [23] S. Dubinsky, A. Korchin, N. Merenkov, G. Pancheri, and O. Shekhovtsova, Eur. Phys. J. C **40**, 41 (2005).
- [24] G. Pancheri, O. Shekhovtsova, and G. Venanzoni, J. Exp. Theor. Phys. **106**, 470 (2008).
- [25] S. Ivashyn, H. Czyz, and A. Korchin, arXiv:0910.5335.
- [26] A. Gallegos, J.L. Lucio, G. Moreno, and M. Napsuciale, arXiv:0908.2192.
- [27] G. Ecker, J. Gasser, A. Pich, and E. de Rafael, Nucl. Phys. B **321**, 311 (1989).
- [28] H. Czyz, A. Grzelinska, and J.H. Kuhn, Phys. Lett. B **611**, 116 (2005).
- [29] G. Isidori, L. Maiani, M. Nicolaci, and S. Pacetti, J. High Energy Phys. 05 (2006) 049.
- [30] A. Bramon, R. Escribano, J.L. Lucio, M.M. Napsuciale, and G. Pancheri, Eur. Phys. J. C **26**, 253 (2002).
- [31] F. Ambrosino *et al.* (KLOE Collaboration), Phys. Lett. B **634**, 148 (2006).
- [32] M. Bando, T. Kugo, S. Uehara, K. Yamawaki, and T. Yanagida, Phys. Rev. Lett. **54**, 1215 (1985).
- [33] M. Bando, T. Kugo, and K. Yamawaki, Phys. Rep. **164**, 217 (1988).
- [34] M. Harada and K. Yamawaki, Phys. Rep. **381**, 1 (2003).
- [35] G. Ecker, J. Gasser, H. Leutwyler, A. Pich, and E. de Rafael, Phys. Lett. B **223**, 425 (1989).
- [36] F.E. Close, N. Isgur, and S. Kumano, Nucl. Phys. B **389**, 513 (1993).
- [37] J. Lucio and J. Pestieau, Phys. Rev. D **42**, 3253 (1990).
- [38] A. Bramon, A. Grau, and G. Pancheri, Phys. Lett. B **289**, 97 (1992).
- [39] J.A. Oller, Phys. Lett. B **426**, 7 (1998).
- [40] P. Beltrame, Ph.D. thesis, Universität Karlsruhe, 2009.